Journal of General Virology (2011), **92**, 2446–2457 **DOI** 10.1099/vir.0.033134-0

Expression profile and subcellular localization of Torque teno sus virus proteins

Laura Martínez-Guinó,[1] Maria Ballester,[1] Joaquim Segalés[1,2] and Tuija Kekarainen[1]

Correspondence
Tuija Kekarainen
tuija.kekarainen@cresa.uab.cat

[1]Centre de Recerca en Sanitat Animal (CReSA), UAB-IRTA, Campus de la Universitat Autònoma de Barcelona, 08193 Bellaterra, Barcelona, Spain

[2]Departament de Sanitat i Anatomia Animals, Universitat Autònoma de Barcelona, 08193 Bellaterra, Barcelona, Spain

In the present study, the expression, generation and subcellular localization of Torque teno sus virus (TTSuV) proteins were characterized into two genetically distinct TTSuV species (TTSuV1 and TTSuV2). Following transfection of three TTSuV1 and TTSuV2 full-length ORF (ORF1, ORF2 and ORF3) expression constructs into porcine kidney cells, alternative splice variants encoding new TTSuV protein isoforms were identified for the first time. Proteins encoded from ORF1 and ORF3 were localized in the nucleoli of porcine kidney cells and that of ORF2 in the cytoplasm and nucleus excluding the nucleoli. The subcellular localization of the different protein isoforms was not only similar between distinct TTSuV species but also to the ones described in human Torque teno virus (TTV). Results of the present *in vitro* study were not based on full-length viral clones but suggested that alternative splicing strategy to generate TTSuV protein isoforms probably occurs *in vivo*. Obtained data provide new information on molecular biology of TTSuV and anelloviruses, which until now has been solely based on results obtained from human TTV.

Received 8 April 2011
Accepted 28 June 2011

INTRODUCTION

The family *Anelloviridae* includes Torque teno viruses (TTVs), which are vertebrate infecting, small, non-enveloped, circular, ssDNA viruses. TTV was first discovered in human and later detected in domestic and wild species including swine (Martínez *et al.*, 2006; Nishizawa *et al.*, 1997). Domestic pig and wild boar-infecting *Torque teno sus virus 1* (TTSuV1) and *Torque teno sus virus 2* (TTSuV2) are classified into the genus *Iotatorquevirus*. It is believed that TTVs might influence the development of some diseases or even modulate the outcome of disease by being present in blood or tissues (Okamoto, 2009). Even a clear-cut pathogenic role for TTSuVs has not been demonstrated to date, its role during co-infection with other pathogens is under debate, especially with regards to porcine circovirus diseases (PCVDs) (Ellis *et al.*, 2008; Kekarainen *et al.*, 2006; Taira *et al.*, 2009).

TTVs share conserved genomic regions with economically important circular ssDNA viruses of swine and poultry [*Porcine circovirus-2* (PCV2) and *Chicken anemia virus* (CAV), respectively] (Biagini, 2009) both members of the family *Circoviridae*. TTSuVs have similar genomic organization with human-infecting TTVs but share less than 45 % nt sequence identity (Niel *et al.*, 2005; Okamoto *et al.*, 2002). Recent studies also demonstrated a high degree of genetic variability between TTSuV1 and TTSuV2 (Cortey *et al.*, 2011). The genome of TTSuV is approximately 2.8 kbp in length and two major potential protein-coding genes, ORF1 and ORF2, can be deduced from the nucleotide sequence. By analogy with related ssDNA viruses, ORF1 is believed to encode the viral capsid protein. ORF2 encodes a non-structural protein, assumed to be involved in viral replication (Hijikata *et al.*, 1999; Huang *et al.*, 2010). TTV ORF2 has also been associated with the NF-κB pathway suppression (Zheng *et al.*, 2007). Analysis of TTSuV nucleotide sequence reveals the existence of an additional ORF, ORF3, generated by splicing and sharing its 5′ end with ORF2. ORF3 is believed to encode a non-structural protein with unknown function (Biagini *et al.*, 2001; Okamoto *et al.*, 2000).

Research on anelloviruses has been based almost solely on PCR techniques. Recently, tissue culture systems supporting human TTV replication, with an inefficient propagation, have been reported (Kakkola *et al.*, 2007; Leppik *et al.*, 2007). To date, few studies have focused on molecular virology, transcription and expression strategies of different human TTV genotypes and results are fairly contradictory. Three mRNAs were produced after transfection with a plasmid containing a TTV genotype 1 genome driven by a putative promoter in COS-1 cells (Kamahora *et al.*, 2000). Moreover, after alternative splicing and alternative translation process, six different proteins from

Supplementary material is available with the online version of this paper.

genotype 6 and seven from isolate P/1C1 (genogroup 1) have been described (Müller *et al.*, 2008; Qiu *et al.*, 2005). Additional splicing events and intragenomic rearrangements of TTVs were identified in lymphoma-derived and T-cell leukaemia cell lines (Leppik *et al.*, 2007). TTV genotype 6 ORF1 and ORF2 proteins were localized in the cytoplasm of transfected cells (Qiu *et al.*, 2005). On the contrary, in a more recent study, ORF1 protein was located in the nucleus (specifically, within the nucleoli), while the ORF3 was observed in the nucleus but not in the nucleolus. In the same study, the ORF2 protein was found, as described previously, in the cytoplasm (Müller *et al.*, 2008). Discrepancies observed between studies suggest that the genomic diversity found in TTV isolates can be associated with different strategies of expression and localization of viral proteins (Müller *et al.*, 2008). It has been suggested that the transcriptional profile of TTSuV would be similar to that found in human TTVs (Okamoto *et al.*, 2002), but experimental evidence is still lacking.

Therefore, the present study was aimed to characterize, for the first time, the generation of different viral proteins of two genetically distant TTSuV species and describe their subcellular localization. For such purpose, TTSuV ORFs were cloned in-frame with the GFP gene and transfected in porcine kidney (PK-15) cells for transcriptional/localization analyses and in human embryonic kidney (HEK 293) cells for localization studies.

RESULTS

Sequence analyses and prediction of TTSuV1 and TTSuV2 viral proteins

The sequence analysis of cloned genes revealed that they corresponded to proposed TTSuV1 type 1C and TTSuV2 to subtype 2A (Huang *et al.*, 2010).

A low level of ORF1 amino acid identity (22–25 %) between TTSuV species has been described (Huang *et al.*, 2010). ORF1 protein of both TTSuV species presented rolling circle replication (RCR)-associated motifs and a conserved arginine-rich N-terminal region similar to those found in CAV and PCV capsid proteins (Mushahwar *et al.*, 1999; Okamoto *et al.*, 1998). Identified RCR motifs were differently presented in TTSuV species as recently described by Huang *et al.* (2010). In TTSuV1-ORF1, motif III (YxxK) (Huang *et al.*, 2010; Müller *et al.*, 2008; Mushahwar *et al.*, 1999) was located at aa position 14–17, while the same motif was not detected in TTSuV2. However, TTSuV2 contained the RCR motif II (HxQ) (Huang *et al.*, 2010; Mankertz *et al.*, 2004) at the C-terminal region of the ORF1 protein (aa position 613–615). All RCR motifs described were conserved in the TTSuV1 or TTSuV2 genomes analysed (Supplementary Fig. S1a, c, available in JGV Online). Motif I (FTL) described in TTV human studies (Müller *et al.*, 2008) was not detected in the TTSuV species.

Bipartite, pat4 and pat7 nuclear localization signals (NLS) were mapped to the N- and C-terminal regions of TTSuV1 and TTSuV2 ORF1 proteins using the PSORT II program (Nakai & Horton, 1999) (Supplementary Fig. S1a, c). The nuclear localization was predicted for ORF1 with a reliability of 76.7 % for TTSuV1 and 70.6 % for TTSuV2.

As described in anelloviruses and CAV (Müller *et al.*, 2008), TTSuV ORF2 contained a protein-tyrosine phosphatase (PTP) motif ($Wx_7Hx_3CxCx_5H$) at aa 9–30 for TTSuV1 and at aa 5–25 for TTSuV2. Except for this conserved motif, the rest of the sequence was not conserved between the viral species. No NLS were detected in ORF2 and subcellular localization of the protein was predicted to be cytoplasmic with a reliability index of 94.1 %.

Pat4 and pat7 NLS were located in the C terminus of TTSuV1 and TTSuV2 ORF3, and bipartite NLS were only predicted for TTSuV2 (Supplementary Fig. S1b, d, available in JGV Online). Subcellular localization was predicted to be nuclear with 94.1 % reliability.

Localization of TTSuV1 and TTSuV2 fusion proteins in transfected cells

As shown in Figs 1 and 2, TTSuV1 and TTSuV2 ORF1 and ORF3 proteins were accumulated in the nucleus 24 h after transfection. Such labelling was found in areas without DAPI staining, mainly corresponding to the nucleolar regions in which perinucleolar heterochromatin clusters were observed. Furthermore, small globular structures were distributed in the nucleoplasm of TTSuV1-ORF1 (Fig. 1, upper panel) and TTSuV2-ORF3 (Fig. 2, lower panel)-transfected cells. Bigger spherical structures were observed in the ORF3-transfected cells compared with those of the ORF1-transfected cells, both resembling nuclear compartments such us splicing speckles or promyelocytic leukaemia (PML) bodies. To confirm a possible co-localization, immunofluorescence experiments were performed using specific antibodies against SC-35 (a marker that specifically labels splicing speckles) and PML bodies (a marker that specially labels human PML bodies). No differences were observed in the distribution of splicing factor SC-35 in PK-15-transfected and non-transfected cells (data not shown), neither co-localization with TTSuV proteins (Figs 1 and 2, last column). Immunofluorescence experiments using the PML body marker were done in HEK 293 cells (Figs 3 and 4) instead of PK-15 cells because of unavailability of anti-pig PML antibody and lack of cross-reactivity with the used PML antibody. First, it was confirmed that the subcellular localization of all ORF proteins were comparable to the ones observed in PK-15 cells (Figs 1–4). Similar globular localization of TTSuV1 ORF1 and TTSuV2 ORF3 as seen in PK-15 cells was also present in transfected HEK 293 cells. Except for TTSuV2 ORF3, none of the proteins were co-localizing with PML bodies. Some globular structures of the TTSuV2 ORF3 protein were adjacent to PML bodies (Fig. 4, last panel).

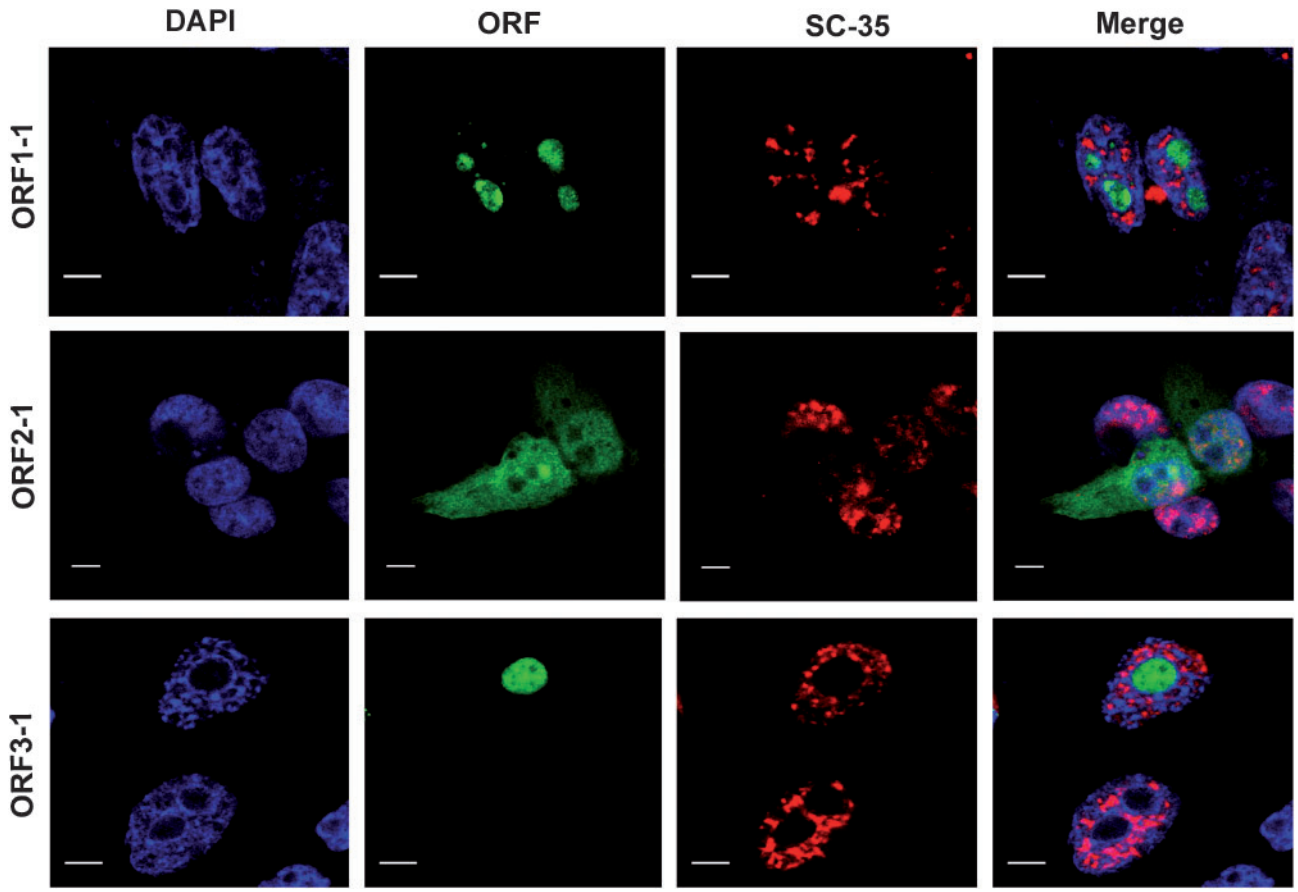

Fig. 1. Subcellular localization of TTSuV1 (ORF1-1, ORF2-1 and ORF3-1) viral proteins in PK-15-transfected cells. Nucleus counterstained with DAPI is shown in blue (first panel), TTSuV proteins fused with GFP are visualized in green (second panel), detection of splicing speckles (SC-35) is shown in red (third panel) and co-localization of markers is shown in the last panel. Bars, 5 μm.

On the contrary, ORF2 protein of both viral species was distributed in the cytoplasm and the nucleus, but never in the nucleoli of PK-15-transfected cells (Figs 1 and 2, middle panels).

To further characterize the encoded proteins, Western blot analysis of TTSuV expressed proteins was performed (Fig. 5). Using anti-GFP antibody, fusion proteins of ORF2 (TTSuV1 36 kDa and TTSuV2 35 kDa) and ORF3 (TTSuV1 53 kDa and TTSuV2 50 kDa) were detected, although with a lower size than expected. However, Western blot analysis of ORF1 protein of both TTSuVs revealed the synthesis of a lower molecular mass (less than 50 kDa) protein, compared with the predicted and expected one of about 100 kDa.

Alternative splicing of TTSuV1 and TTSuV2 RNAs

Due to the unexpected size of the TTSuV ORF1 protein characterized by Western blot, possible splicing variants of each cloned full-length ORF were examined. Several combinations of primers were used in RT-PCR (Supplementary Table S1, available in JGV Online). GFP-transfected cells were also RT-PCR tested and results were negative in all primer combinations applied (data not shown). Table 1 summarizes the characteristics of splicing sites of TTSuV1 and TTSuV2 ORF after sequencing the obtained amplicons and the confidence of splicing sites as predicted using the NetGene 2 program.

For ORF1, no amplification of the expected full-length ORF1 transcript was obtained. However, two and three spliced transcripts for TTSuV1 and TTSuV2, respectively, were amplified and sequenced (Fig. 6a, b). Alternatively spliced TTSuV1 ORF1 transcripts were named as ORF1-1A and ORF1-1B, ORF1-1A being the most abundant variant (Fig. 6a). Transcript ORF1-1A contained one intron, which was spliced between nt 118 and 1512. Transcript ORF1-1B was smaller than ORF1-1A and contained two introns; one between nt 64 and 1511 and the other one between nt 1658 and 1732 (Fig. 6a). Regardless of the splicings, the reading frame was maintained generating two protein isoforms, namely ORF1-1A (181 aa) and ORF1-1B (142 aa), still in-frame with GFP. Three different transcripts, ORF1-2A,

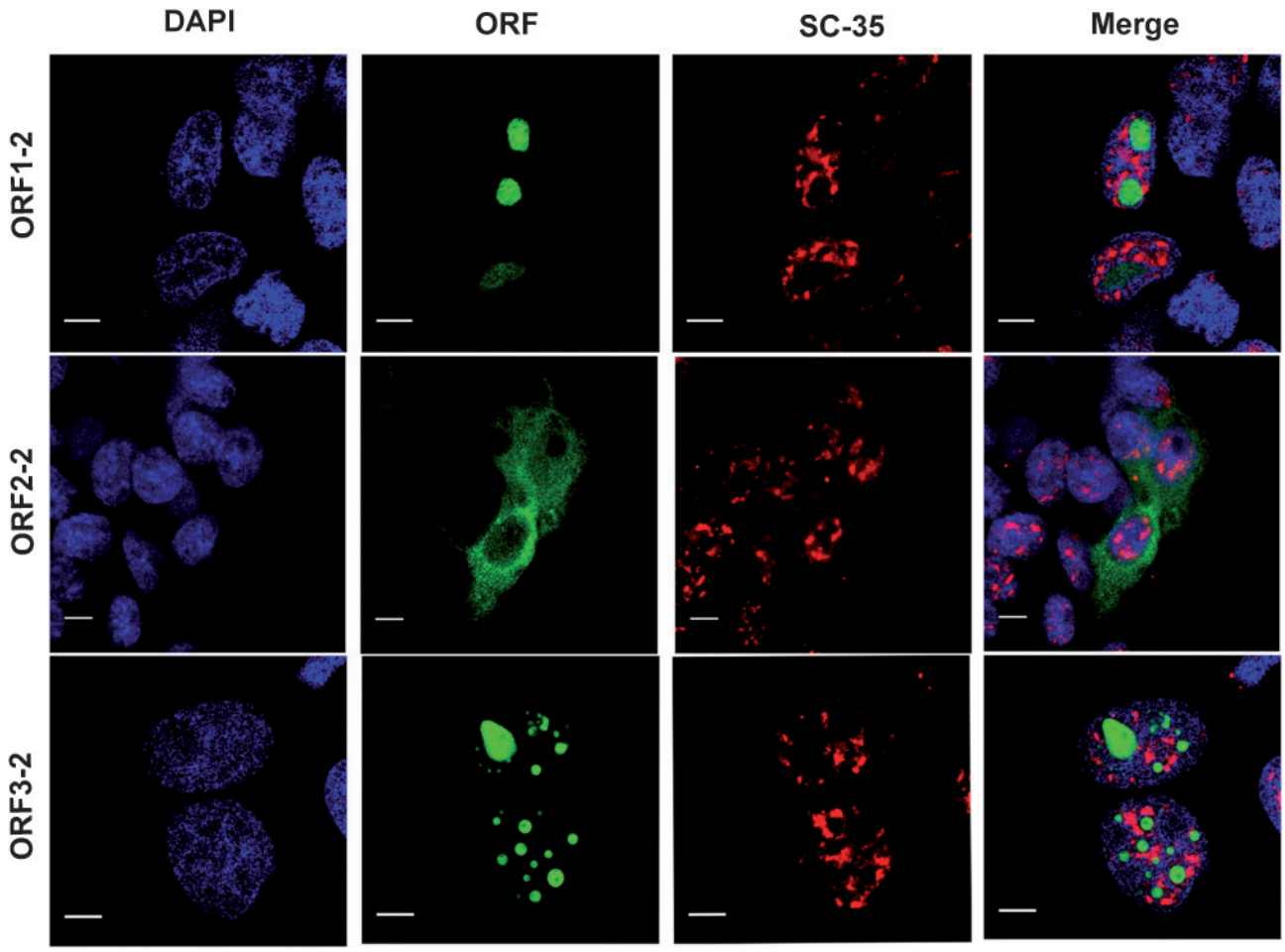

Fig. 2. Subcellular localization of TTSuV2 (ORF1-2, ORF2-2 and ORF3-2) viral proteins in PK-15-transfected cells. Nucleus counterstained with DAPI is shown in blue (first panel), TTSuV proteins fused with GFP are visualized in green (second panel), detection of slicing speckles (SC-35) is shown in red (third panel) and co-localization of markers is shown in the last panel. Bars, 5 μm.

ORF1-2B and ORF1-2C, were generated by alternative splicing from the full-length TTSuV2 ORF1 (Fig. 6b). ORF1-2A sequence revealed the largest transcript containing one intron spliced between nt 121 and 1458. Transcript ORF1-2B had the same intron described in transcript ORF1-2A and an extra intron located at nt 1573 and 1663. Finally, ORF1-2C was the smallest transcript and had one intron between nt 121 and 1663 (Fig. 6b). The translation of these transcripts generated three different protein isoforms of 176, 138 and 100 aa, respectively, and revealed that ORF1-2B and ORF1-2C had a different reading frame in the C terminus compared with the one observed in ORF1-2A (Fig. 6b), the only one in-frame with GFP. ORF2 transcripts obtained for both TTSuV species were of predicted full-length size and no splicing events were detected.

Since TTSuV ORF1 and ORF3 are overlapping genes and ORF3 5′-end is shared with ORF2, the sequence analysis of TTSuV ORF3 transcripts revealed identical splicing sites described for TTSuV ORF1 (Table 1). For TTSuV1, the predicted truncated ORF3 amplicon was obtained (ORF3-1) (Fig. 6c), while three different transcripts were amplified for TTSuV2 (Fig. 6d). ORF3-2A generated the expected truncated TTSuV2 ORF3 protein of around 196 aa, while ORF3-2B and ORF3-2C generated two different proteins of 166 and 128 aa in length, respectively, with a common reading frame but different from the one observed for the ORF3-2A protein (Fig. 6d).

Spliced donor and acceptor positions described for TTSuV1 and TTSuV2 were highly conserved in full-length genomes analysed (Supplementary Fig. S2, available in JGV Online). Although TTSuV1 is divided into three different types (Cortey *et al.*, 2011; Huang *et al.*, 2010) with nucleotide identity ranging from 65 to 99 %, donor and acceptor positions that generated the ORF1-1A isoform and ORF3-1 truncated protein were conserved. On the contrary, not all the sites described for ORF1-1B isoform were conserved between TTSuV1 types (Supplementary Fig. S2a).

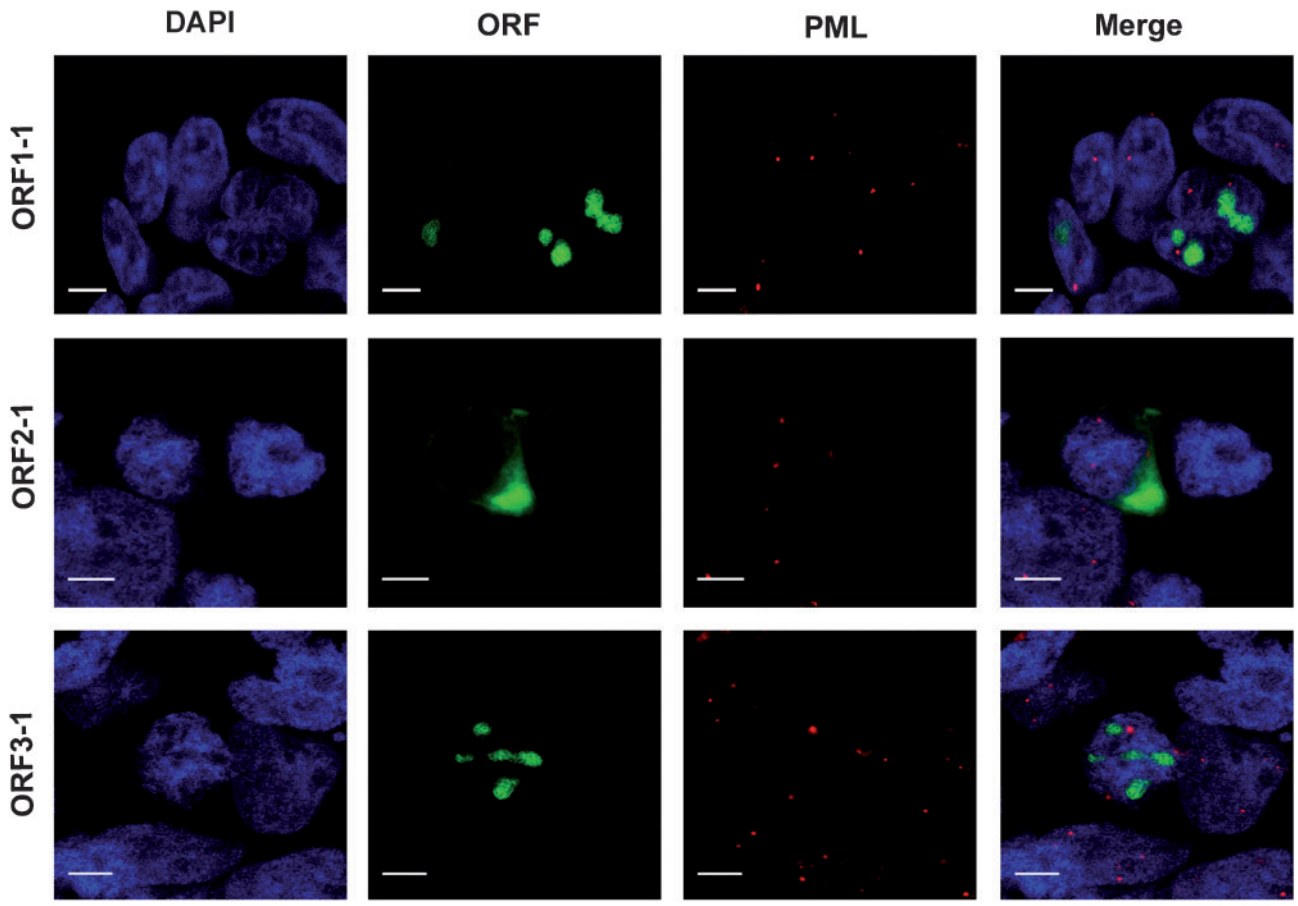

Fig. 3. Subcellular localization of TTSuV1 (ORF1-1, ORF2-1 and ORF3-1) viral proteins in HEK 293-transfected cells. Nucleus counterstained with DAPI is shown in blue (first panel), TTSuV proteins fused with GFP are visualized in green (second panel), detection of PML bodies is shown in red (third panel) and co-localization of markers is shown in the last panel. Bars, 5 μm.

TTSuV2 full-length genome sequences are more identical (from 82 to 99 %) than TTSuV1 genomes, and donor and acceptors splicing sites were maintained between subtypes (Cortey *et al.*, 2011; Huang *et al.*, 2010) with a nucleotide identity ranging from 80 to 100 % (Supplementary Fig. S2b).

Isoform diversity at the amino acid level determined that for ORF1-1A and ORF1-1B the amino acid sequence identity observed between viral types 1a, 1b and 1c ranged from 51 to 100 % and from 52 to 100 %, respectively. In the case of TTSuV2 genomes, the amino acid sequence identity was higher than TTSuV1 (ORF1-2A from 89 to 99 %, ORF1-2B from 86 to 100 %, ORF1-2C from 87 to 100 %, ORF3-2A from 83 to 100 %, ORF3-2B from 80 to 100 % and ORF3-2C from 86 to 100 %).

Subcellular localization of TTSuV1 and TTSuV2 protein isoforms

To study specifically the subcellular localization of the different protein isoforms, alternatively spliced transcripts, amplified from cDNA (thus no introns were present) were cloned in-frame with GFP, transfected into PK-15 cells and analysed by confocal microscopy. No differences between ORF1-1A and ORF1-1B distribution were observed and both proteins were located in DAPI-depleted areas, most probably corresponding to nucleolar regions (Fig. 7a). However, small globular foci were only seen in the nucleoplasm of cells transfected with the ORF1-1B spliced variant.

The same observation was made when the localization of the different transcripts generated from TTSuV2 ORF1 was studied. All isoforms were localized in nucleolar areas of transfected cells (Fig. 7b). Different localization was determined between ORF3-2 isoforms (Fig. 7c). Predicted truncated ORF3-2A protein was located in globular foci in the nucleoplasm of transfected cells, while ORF3-2B and ORF3-2C proteins localized mainly in nucleoli.

DISCUSSION

The lack of techniques other than PCR or quantitative PCR has limited TTSuV research to epidemiological studies. To

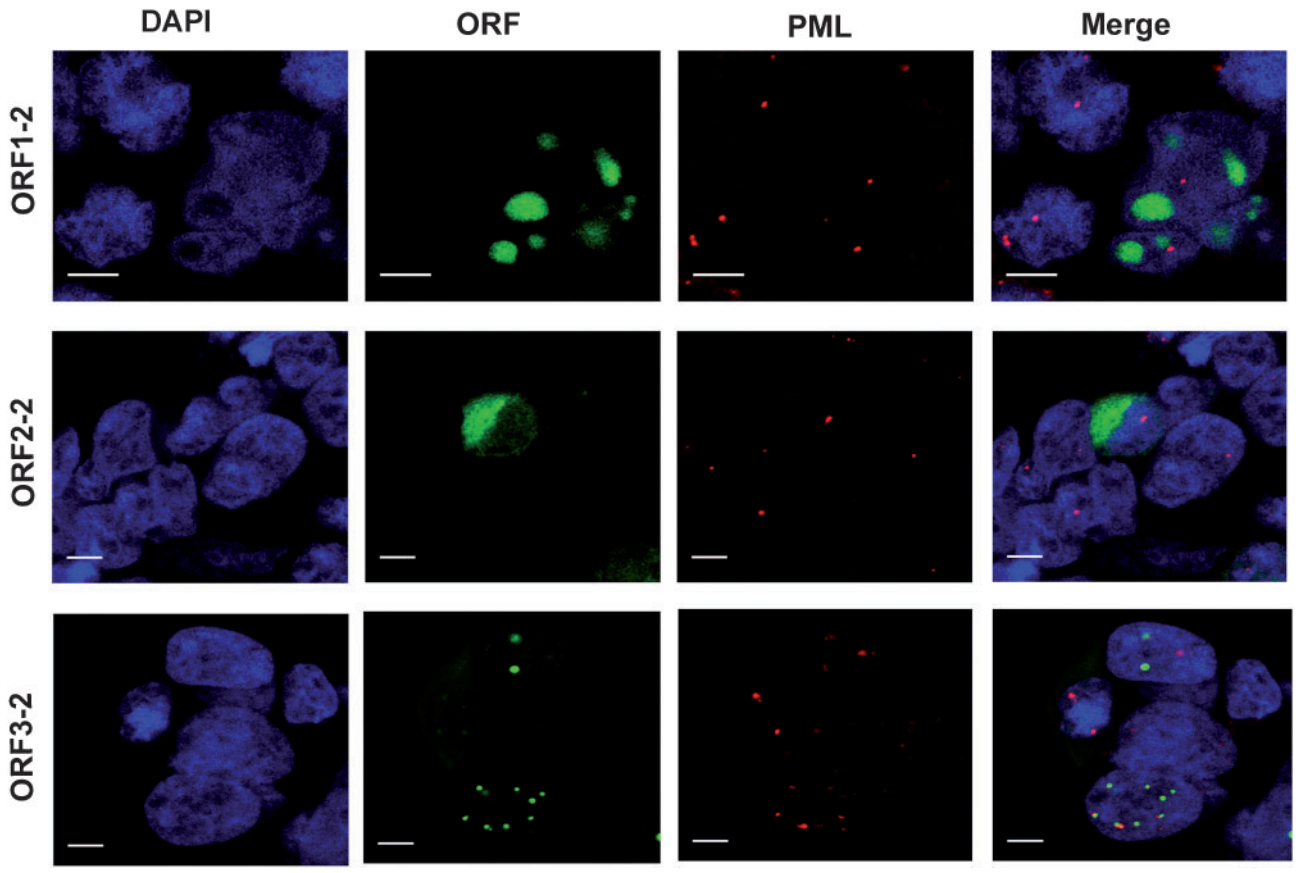

Fig. 4. Subcellular localization of TTSuV2 (ORF1-2, ORF2-2 and ORF3-2) viral proteins in HEK 293-transfected cells. Nucleus counterstained with DAPI is shown in blue (first panel), TTSuV proteins fused with GFP are visualized in green (second panel), detection of PML bodies is shown in red (third panel) and co-localization of markers is shown in the last panel. Bars, 5 μm.

improve existing knowledge on molecular properties of TTSuV, the present study investigated the characteristics of TTSuV1 and TTSuV2 ORFs by studying their transcription and protein expression and localization.

The transcriptional analysis indicated that TTSuV uses a strategy of alternative splicing to generate ORF1 and ORF3 protein isoforms. According to obtained results, the full-length, non-spliced ORF1 mRNA is not produced, but two (ORF1-1A and ORF1-1B) and three alternatively spliced (ORF1-2A, ORF1-2B and ORF1-2C) mRNAs were detected in TTSuV1 and TTSuV2, respectively. Interestingly, although the splicing of TTSuV1 ORF1 generated two isoform proteins of different size, the reading frame and, therefore, the encoded amino acid sequence did not change. Accordingly, when ORF1-1 was analysed by Western blot, the full-length predicted protein was not detected; instead, it revealed a 50 kDa protein, most probably corresponding to both ORF1-1 isoforms, very similar in molecular mass and difficult to discriminate by the analysis performed. The C terminus of TTSuV2 ORF1 and ORF3 protein isoforms varied depending on the splicing site used, being different in amino acid composition between ORF1-2A and ORF1-2B/2C or ORF3-2A and ORF3-2B/C. The difference observed affected the reading frame and resulting isoforms were out of frame with GFP and, therefore, not detected by Western blot analysis. For this reason, the protein detected by Western blot corresponded to the ORF1-2A and ORF3-2A protein isoform described.

For both viral species, the differences in RT-PCR band intensities observed between the different spliced variants and the undetected full-length ORF1 indicated that there were different efficiencies of splicing depending on the site. The expression of the full-length protein cannot be definitively ruled out; however, according to obtained *in vitro* results, it would not be the main one detected. Similar differences in the abundance of ORF1 isoforms have been described in human TTV (Müller *et al.*, 2008) and also in other circular ssDNA viruses like porcine circovirus-1 (PCV1) (Mankertz & Hillenbrand, 2001), although the full-length protein derived from non-spliced mRNA was also detected by Western blot in TTV human studies (Müller *et al.*, 2008). It might be that ORF1 TTSuV protein was not expressed, that the protein was unstable and degraded fast, as has been already suggested in human studies (Qiu *et al.*, 2005), or that the techniques used were

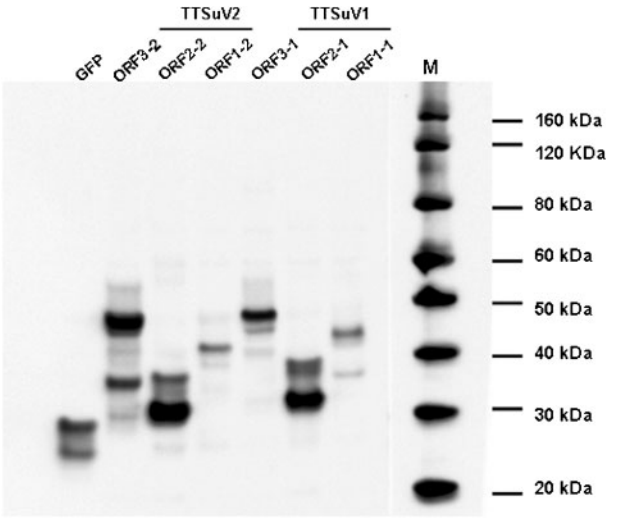

Fig. 5. Western blot analysis of expressed fused TTSuV proteins using anti-GFP antibody. The lanes show, from left to right, pGFP, pORF3-2–GFP, pORF2-2–GFP, pORF1-2–GFP, pORF3-1–GFP, pORF2-1–GFP, pORF1-1–GFP, BenchMark His-tagged protein standard (Invitrogen Corporation) (M).

not sensitive enough for its detection. Due to unavailability of a cell culture system for virus propagation, the generated data were not based on transfection of full-length TTSuV clones or natural infection assay. Therefore, it is possible that obtained results would differ from the natural viral infection. However, in a human study, where comparison of virus mediate and transient expression of ORF1 was performed, no differences were observed (Müller *et al.*, 2008). Also, preliminary results from our laboratory indicate that TTSuV gene splicing occurs in tissues of naturally infected pigs (data not shown). Currently, it is not possible to confirm the *in vivo* expression of TTSuV proteins due to the lack of antibodies. Furthermore, sequence analysis of all published TTSuV genomes also demonstrates that the splicing donor and acceptor sites described for the generation of protein isoforms are highly maintained between different TTSuV1 types and TTSuV2 subtypes.

Subcellular localization analysis of expressed proteins demonstrated that proteins of genetically distinct TTSuV species localized in the same cellular compartments. ORF1 and ORF3 proteins localized to the nucleus and nucleolus of PK-15 cells and the ORF2 protein was distributed in the cytoplasm and nucleus, but never in the nucleoli. Indeed, several nuclear and nucleolar localization signals (NLS/NoLS) were identified in the N terminus of TTSuV1 and TTSuV2 ORF1 and C-terminal part of ORF3. Furthermore, similar localization of the human TTV proteins has been described previously (Müller *et al.*, 2008). Noteworthy, in spite of the high degree of amino acid divergence (>50 %) between human and swine TTVs, viral protein localization is not altered and seems to be maintained in the family *Anelloviridae*.

The nucleolus is the largest nuclear compartment involved in crucial cell biology functions and it has been suggested that viruses can interact with it to support important viral processes like transcription, translation and replication (Hiscox, 2002). Being DNA viruses with a small genome size, anelloviruses are dependent on the nuclear host factors for their expression and replication. Therefore, TTSuV nuclear localization of ORF1 and ORF3 may be indicative of the putative implication of those proteins in basic viral processes. Based on similarities with other ssDNA viruses, it has been proposed that a rolling circle mechanism is used for virus replication (Mushahwar

Table 1. TTSuV mRNA transcripts obtained following splicing

Nucleotide position and splicing donor and acceptor site localization from full-length protein sequence. Confidence value predicted by the NetGene2 program. ND, Not detected.

Species	Protein isoform	Nucleotide position	Splicing donor site sequence	NetGene2 confidence value	Nucleotide position	Splicing acceptor site sequence	NetGene2 confidence value
TTSuV1	ORF1-1A	118	ACGTCGGCGG	0.95	1512	TTCGGCGGCA	0.43
	ORF1-1B	65	GGAGACGTCG	ND	1511	GTTCGGCGGC	ND
		1658	GGAGCTCAAG	0.82	1732	AACCAAAGGA	0.18
	ORF3-1A	216	ACGTCGGCGG	0.95	1610	TTCGGCGGCA	0.43
TTSuV2	ORF1-2A	121	CCGCGCAAAG	0.99	1458	TGGGGAGGAC	0.17
	ORF1-2B	121	CCGCGCAAAG	0.99	1458	TGGGGAGGAC	0.17
		1573	CCCCTCCAAG	0.80	1663	AGACAGAGGA	0.43
	ORF1-2C	121	CCGCGCAAAG	0.99	1663	AGACAGAGGA	0.43
	ORF3-2A	204	CCGCACAAAG	1.00	1541	TGGGGAGGAC	0.17
	ORF3-2B	204	CCGCACAAAG	1.00	1541	TGGGGAGGAC	0.17
		1656	CCCCTCCAAG	0.80	1746	AGACAGAGGA	0.43
	ORF3-2C	204	CCGCACAAAG	1.00	1746	AGACAGAGGA	0.43

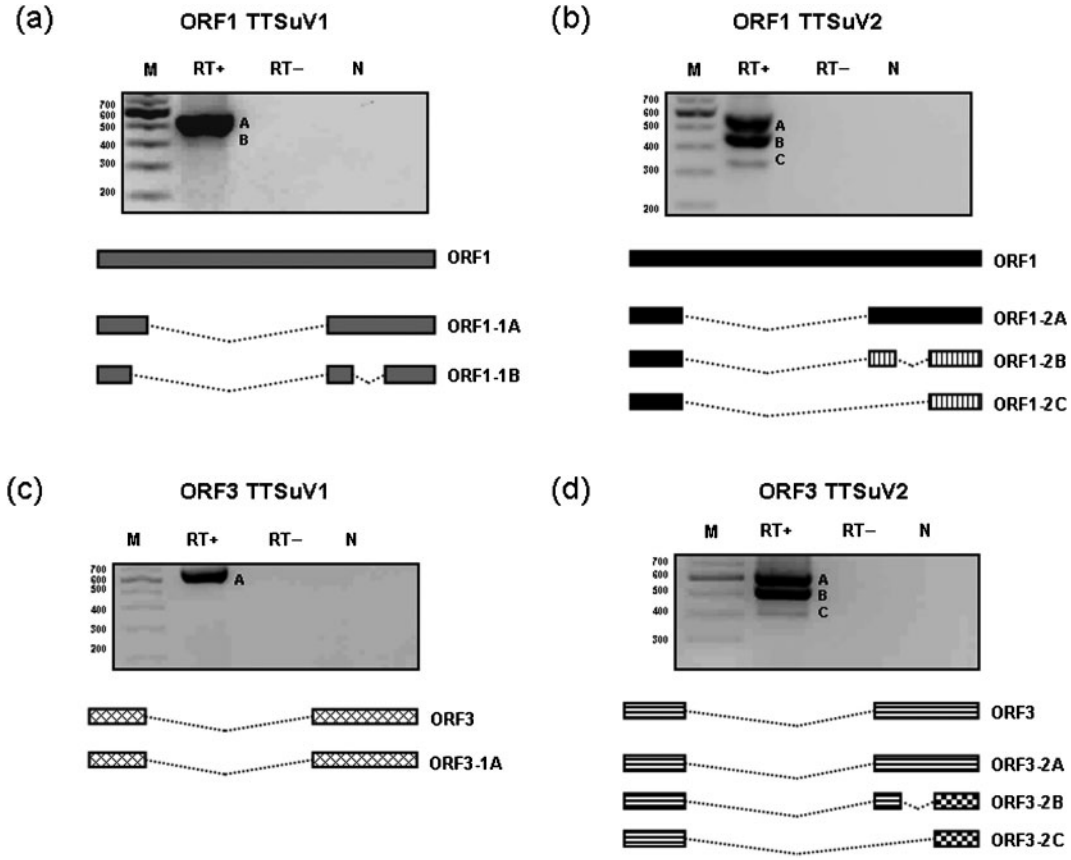

Fig. 6. RT-PCR amplification and schematic presentation of TTSuV1 (a, c) and TTSuV2 (b, d) alternative splicing of ORF1 (a, b) and ORF3 (c, d). Amplicons corresponding to the different protein isoforms are indicated in the left of each panel, amplified transcript (RT+), RT-negative control (RT–) and PCR-negative control (N). Expected full-length protein is depicted on top of the schematic representation, below are depicted the detected alternatively spliced RNAs (dotted lines represent introns). Encoded proteins are presented as boxes; different patterns of boxes reflect different amino acid sequences between protein isoforms. DNA size-marker, 100 bp (M).

et al., 1999), with ORF1 containing the conserved RCR motifs. Viral packaging has also been attributed to ORF1 protein (Erker *et al.*, 1999; Hijikata *et al.*, 1999). TTSuV ORF3 protein also contained NLS/NoLs signals that target it to the nucleolus, but did not contain RCR motifs. In human studies, ORF3 protein function has been associated with apoptosis based on similarities observed with VP3 protein from closely related CAV (Kooistra *et al.*, 2004); such similarities were not found in TTSuV proteins.

TTSuV ORF2 protein did not contain NLS, which was in accordance with its localization mainly in cytoplasm. Due to a small size, ORF2 can diffuse into the nucleus. ORF2 viral protein function has been related to tyrosine phosphatase (PTPases) activity, described to be involved in viral replication (Hijikata *et al.*, 1999; Huang *et al.*, 2010). However, without the possibility of purifying the virus and not having an efficient culture system supporting TTSuV replication, the functional implication of TTSuV proteins remains unclear.

In the present study, TTSuV1 ORF1 and TTSuV2 ORF3 genes were also localized as foci of variable sizes throughout the nucleoplasm of transfected cells. In both protein isoforms obtained from the full-length TTSuV1 ORF1 protein, the reading frame with the GFP gene was not affected and both proteins were generated. Simultaneous expression is feasible, so it was not possible to discriminate between them in the images obtained from TTSuV1 ORF1 full-length gene construct. This hypothesis was confirmed when ORF1-1 protein isoforms localization was studied. A different pattern between ORF1-1A and ORF1-1B was observed; the former one was detected in the nucleolus, while the latter one in the nucleolus but also forming evident globular foci in the nucleoplasm.

In the case of TTSuV2 ORF3, the splicing strategy altered the reading frame; ORF3-2B and ORF3-2C protein isoforms shared a common reading frame different from the one observed for ORF3-2A (expected truncated protein). Furthermore, ORF3-2A was detected as globular structures in the nucleoplasm, while ORF3-2B and ORF3-2C isoforms

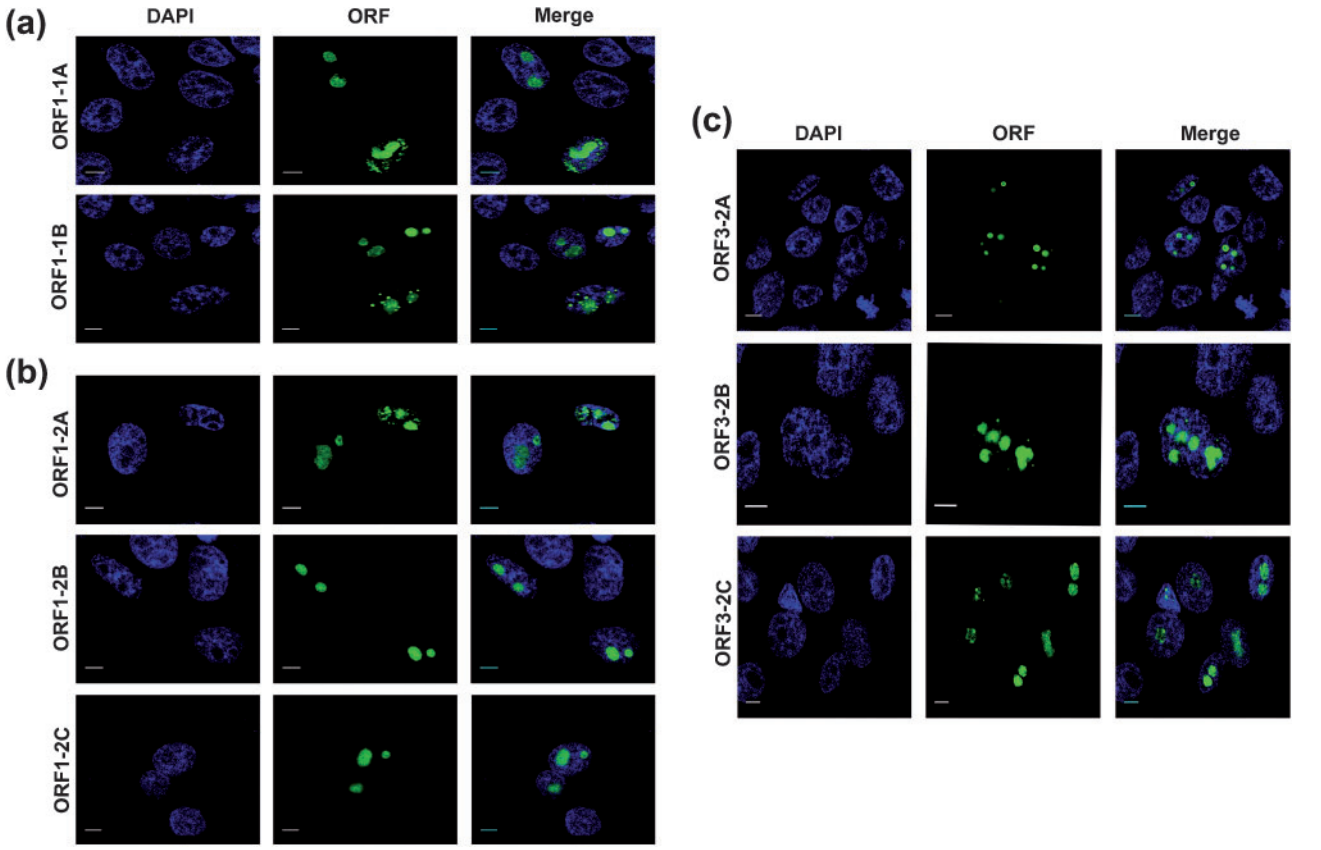

Fig. 7. Subcellular localization of TTSuV1 and TTSuV2 viral protein isoforms. (a) TTSuV1 ORF1 protein isoforms, (b) TTSuV2 ORF1 protein isoforms and (c) TTSuV2 ORF3 protein isoforms. Nuclei counterstained with DAPI are shown in blue (first panel), TTSuV proteins fused with GFP are visualized in green (second panel). Merged view is shown in the last panel. Bars, 5 μm.

were localized in the nucleolus. In a recent study, human TTV genogroup 1 ORF2 protein was detected in similar granular structures within the nucleus and the authors suggested its distribution to nuclear speckles (Müller *et al.*, 2008). Pre-mRNA splicing factors are localized in nuclear speckles, subnuclear dynamic organelles found in the nucleoplasm of mammalian cells that are involved in assembly and/or modification of splicing factors and functionally related with gene expression (Spector & Lamond, 2011). To determine if TTSuV proteins were co-localized with nuclear speckles, PK-15 cells expressing GFP fusion proteins of TTSuVs were immunostained with the primary mouse mAb against SC-35 and observed by confocal microscopy. According to the size and shape, globular deposits could correspond to aggregation of misfolded protein. The formation of protein aggregates is a dynamic process that cells use to deal with misfolded protein resulting from cell stress, overexpresion of proteins or viral infection (Fu *et al.*, 2005; Kopito, 2000). Protein aggregates have also been associated with PML bodies. There are subnuclear structures involved mainly in three general functions like nucleoplasmic protein level regulation, post-translation modification and protein degradation and also with DNA repair (Ching *et al.*, 2005). Additionally, many viruses use PML bodies to concentrate viral protein to facilitate replication and assembly (Wileman, 2007). To confirm this hypothesis, co-localization was studied in TTSuV expression construct transfected HEK 293 cells, which were immunolabelled with the PML antibody prior to confocal microscopy analysis. While globular foci of TTSuV1 ORF1 and TTSuV2 ORF3 were not co-localizing with PML, TTSuV2 ORF3 protein was closely associated with PML bodies. It is difficult to give an explanation on this situation, especially because the TTSuV ORF3 protein role is still unknown. However, in other nuclear replicating viruses PML bodies have been associated with protein aggregates, viral replication and site of viral assembly (Wileman, 2007). Further studies are needed to elucidate the functional role of ORF3 during TTSuV infection.

In summary, this is the first study describing the alternative splicing pattern and protein isoforms generated of two genetically distinct TTSuV species. Furthermore, their subcellular localization and association with nuclear speckles and PML bodies are described. These results open new perspectives in understanding the molecular mechanisms involved during TTSuV infection.

METHODS

Computer analysis of TTSuV1 and TTSuV2 viral proteins. *In silico* analysis of TTSuV viral proteins cellular localization was done by the PSORT II program, http://psort.hgc.jp/ (Nakai & Horton, 1999). To predict possible functional motifs in TTSuV proteins, the Eukaryotic Linear Motif (ELM) program (http://elm.eu.org/) was applied. The NetGene2 program was used to predict splicing sites in TTSuV genes (Brunak *et al.*, 1991) (http://www.cbs.dtu.dk/services/NetGene2/). Conservation of described motifs and predicted splicing sites were studied by the alignment of amino acid and DNA sequences of swine full-length available genomes in GenBank of TTSuV1 and TTSuV2 using the CLUSTAL W program. The amino acid diversity of TTSuV protein isoforms described was analysed using sequence identity matrix in the BioEdit Sequencer Alignment Editor V 7.0.5 program comparing deduced amino acid isoform sequences in all TTSuV1 and TTsuV2 genomes available.

Cell culture. PK-15 cells that tested negative for PCV1, PCV2 and TTSuVs were grown in minimal essential medium (Gibco) supplemented with 10 % FBS (Gibco) at 37 °C in a 5 % CO_2 humidified atmosphere.

HEK 293 cells that tested negative for TTSuVs were grown in Dulbecco's modified Eagle's medium (Gibco) supplemented with 10 % FBS (Gibco) at 37 °C in a 5 % CO_2 humidified atmosphere.

Cell passaging was done with TrypLE express (Invitrogen Corporation) to avoid any contamination with porcine-derived trypsin (Kekarainen *et al.*, 2009).

ORF amplification and plasmid construction. Full-length ORF1, ORF2 and ORF3 from TTSuV1 (ORF1-1, ORF2-1 and ORF3-1) and TTSuV2 (ORF1-2, ORF2-2 and ORF3-2) genomes were PCR amplified from TTSuV-positive serum sample, which was previously shown to be positive by diagnostic PCR (Segalés *et al.*, 2009). The primers to amplify ORFs were designed based on the TTSuV1 (GenBank accession no. GU570202) and TTSuV2 sequences (GenBank accession no. AY823991) (Supplementary Table S1). Amplification products were cloned into pcDNA3.1/CT–GFP-TOPO expression vector (Invitrogen). For TTSuV1 ORF1 and ORF3 amplification, an initial denaturing step at 94 °C for 5 min, followed by 25 cycles at 94 °C for 15 s, 55 °C for 15 s and 68 °C for 2 min with a final extension at 72 °C for 10 min was performed. For TTSuV1 and TTSuV2 ORF2 amplification, PCR conditions were identical but with an extension at 68 °C for 30 s. For TTSuV2 ORF1 and ORF3 amplification, conditions used were an initial DNA denaturation at 94 °C for 5 min, followed by 35 cycles at 94 °C for 20 s, 55 °C for 15 s and 72 °C for 1 min, with a final extension at 72 °C for 10 min. Amplification products were run on a 1.8 % TAE-agarose gel, purified using NucleoSpin Extract II (Macherey-Nagel) and ligated into pcDNA3.1/CT–GFP-TOPO expression vector to generate TTSuV proteins in-frame with the GFP (pORF1-1–GFP, pORF2-1–GFP, pORF3-1–GFP, pORF1-2–GFP, pORF2-2–GFP and pORF3-2–GFP). Correct clones were confirmed by sequencing both strands of the insert using primer sites located in the vector. Sequencing reactions were done using Big Dye Terminator v3.1 cycle sequencing kit (Applied Biosystems) and run using ABI Prism 3100 sequencer analyser (PerkinElmer). Sequences were verified, edited and aligned using the Vector NTI program (Invitrogen). Identification of the TTSuV type/subtype was done based on phylogenetic analysis of obtained sequences according to Huang *et al.* (2010).

Transfection and RNA extraction. A total of 2.5×10^5 PK-15 cells were cultured into six-well plates and grown overnight until 70–80 % confluence before transfection. Cells were then transfected with 1.5 μg of the TTSuV ORF expression constructs using 5 μl of Transfectin Lipid Reagent (Bio-Rad Laboratories). Non-transfected PK-15 cells served as negative control and cells transfected with plasmid encoding the GFP gene (pGFP) as positive control of expression. Total RNA was extracted 24 h post-transfection using Trizol Reagent (Invitrogen). Briefly, cells were disrupted using 600 μl Trizol Reagent and 120 μl 1-bromo-3-chloropropane (Sigma). The suspension obtained was centrifuged at 12 000 ***g*** at 4 °C for 15 min and the aqueous face formed was separated prior to being precipitated with 300 μl 100 % isopropyl alcohol and centrifuged at 12 000 ***g*** at 4 °C for 10 min. The resulting RNA pellet was washed with 1 ml 75 % ethanol and air-dried. RNA was dissolved in RNase-free water and contaminating DNA was removed using Turbo DNA-free kit (Ambion).

RT-PCR analysis. Five hundred nanograms of obtained RNA was converted to cDNA using the SuperScript II Reverse Transcriptase (RT) System (Invitrogen) according to the manufacturer's protocol. Negative RT control was performed using sterile water instead of SuperScript II RT. GFP-transfected cells were used as a negative control in the RT-PCR assay. To characterize the alternative splicing of studied genes, PCRs were performed using viral-specific primer pairs (Supplementary Table S1). Splicing variants obtained were subcloned into pcDNA3.1/CT–GFP-TOPO expression vector (Invitrogen) and sequenced as described above.

Western blot analysis. After 24 h post-transfection with TTSuV1 or TTSuV2, PK-15 cells were washed with 1 × PBS and then lysed in cold buffer (which included 50 mM Tris-HCl, pH 8, 150 mM NaCl, 2 mM EDTA, 10 % Triton X-100 and protease inhibitor cocktail). After centrifugation at 12 000 ***g*** for 15 min at 4 °C, supernatants were collected. Ten microlitres was run in denaturing conditions in NuPage Novex 4–12 % Bistris gel (Invitrogen) and electroblotted to a Hybond ECL nitrocellulose membrane (GE Healthcare). The membrane was blocked with ECL Advance Blocking Agent (Amersham Bioscience) and incubated with an anti-GFP rabbit antibody (Invitrogen), followed by addition of HRP conjugated with anti-rabbit IgG (Sigma-Aldrich). Obtained proteins were detected by ECL Advance Western blotting detection kit (Amersham Biosciences) and visualized by using Fluorochem HD2 chemiluminescencent workstation (Alpha Innotech).

Fluorescence microscopy. A total of 2.5×10^5 PK-15 or 2×10^5 HEK 293 cells cultured on glass coverslips in six-well plates were transfected with expression vectors. Twenty-four hours post-transfection, cells were washed with 1 × PBS and fixed with 4 % paraformaldehyde (PFA) for 10 min at room temperature. For the detection of the SC-35 splicing speckle nuclear marker, PK-15 cells were permeabilized with 0.5 % Triton X-100 for 15 min at room temperature and washed with 1 × PBS for 5 min prior to being blocked with 3 % BSA–1 × PBS solution for 1 h at room temperature. Cells were then incubated with the primary mouse mAb against SC-35 (1 : 500; Sigma-Aldrich) for 1 h in blocking solution at room temperature. After three washes with 1 × PBS, cells were incubated with Cy3-conjugated anti-IgG_1 mouse antibody (1 : 500; Jackson Immunoresearch Europe) for 1 h in blocking solution at room temperature. For the PML bodies detection, HEK 293 cells were treated as described above but were incubated with the primary mouse mAb N-terminal epitope of human PML (PG-M3) SC-966 (1 : 10; Santa Cruz Biotechnology) for 1 h in blocking solution at room temperature. Finally, nuclei were counterstained with DAPI (1 μg ml^{-1}) and coverslips were mounted with Fluoprep (bioMérieux). Fluorescence images were viewed on a Nikon eclipse 90i epifluorescence microscope equipped with a DXM 1200F camera (Nikon Corporation). Image stacks were captured using the Leica TCS SP5 confocal microscope (× 40/NA 1.25 objective). Images were processed by using the LAS AF Lite program from Leica and Image J v1.44e software (http://rsb.info.nih.gov/ij).

ACKNOWLEDGEMENTS

The authors thank Fernando Rodríguez (CReSA) for his scientific input, and Alexandra Jimenez-Melsió and Anna M. Llorens from CReSA for their technical assistance. This work was funded by the Spanish government, grants AGL2006-02778/GAN, TRT2006-00018 and CONSOLIDER-PORCIVIR CSD2006-00007. T. K. was supported by the Ramon y Cajal and M. B. by a Juan de la Cierva contract from the Spanish Ministry of Science and Innovation.

REFERENCES

Biagini, P. (2009). Classification of TTV and related viruses (anelloviruses). *Curr Top Microbiol Immunol* **331**, 21–33.

Biagini, P., Gallian, P., Attoui, H., Touinssi, M., Cantaloube, J.-F., de Micco, P. & de Lamballerie, X. (2001). Genetic analysis of full-length genomes and subgenomic sequences of TT virus-like mini virus human isolates. *J Gen Virol* **82**, 379–383.

Brunak, S., Engelbrecht, J. & Knudsen, S. (1991). Prediction of human mRNA donor and acceptor sites from the DNA sequence. *J Mol Biol* **220**, 49–65.

Ching, R. W., Dellaire, G., Eskiw, C. H. & Bazett-Jones, D. P. (2005). PML bodies: a meeting place for genomic loci? *J Cell Sci* **118**, 847–854.

Cortey, M., Macera, L., Segalés, J. & Kekarainen, T. (2011). Genetic variability and phylogeny of *Torque teno sus virus* 1 (TTSuV1) and 2 (TTSuV2) based on complete genomes. *Vet Microbiol* **148**, 125–131.

Ellis, J. A., Allan, G. & Krakowka, S. (2008). Effect of coinfection with genogroup 1 porcine Torque teno virus on porcine circovirus type 2-associated postweaning multisystemic wasting syndrome in gnotobiotic pigs. *Am J Vet Res* **69**, 1608–1614.

Erker, J. C., Leary, T. P., Desai, S. M., Chalmers, M. L. & Mushahwar, I. K. (1999). Analyses of TT virus full-length genomic sequences. *J Gen Virol* **80**, 1743–1750.

Fu, L., Gao, Y. S., Tousson, A., Shah, A., Chen, T. L., Vertel, B. M. & Sztul, E. (2005). Nuclear aggresomes form by fusion of PML-associated aggregates. *Mol Biol Cell* **16**, 4905–4917.

Hijikata, M., Iwata, K., Ohta, Y., Nakao, K., Matsumoto, M., Matsumoto, H., Kanai, K., Baba, K., Samokhvalov, E. I. & Mishiro, S. (1999). Genotypes of TT virus (TTV) compared between liver disease patients and healthy individuals using a new PCR system capable of differentiating 1a and 1b types from others. *Arch Virol* **144**, 2345–2354.

Hiscox, J. A. (2002). The nucleolus–a gateway to viral infection? *Arch Virol* **147**, 1077–1089.

Huang, Y. W., Ni, Y. Y., Dryman, B. A. & Meng, X. J. (2010). Multiple infection of porcine Torque teno virus in a single pig and characterization of the full-length genomic sequences of four U.S. prototype PTTV strains: implication for genotyping of PTTV. *Virology* **396**, 289–297.

Kakkola, L., Tommiska, J., Boele, L. C. L., Miettinen, S., Blom, T., Kekarainen, T., Qiu, J., Pintel, D., Hoeben, R. C. & other authors (2007). Construction and biological activity of a full-length molecular clone of human Torque teno virus (TTV) genotype 6. *FEBS J* **274**, 4719–4730.

Kamahora, T., Hino, S. & Miyata, H. (2000). Three spliced mRNAs of TT virus transcribed from a plasmid containing the entire genome in COS1 cells. *J Virol* **74**, 9980–9986.

Kekarainen, T., Sibila, M. & Segalés, J. (2006). Prevalence of swine Torque teno virus in post-weaning multisystemic wasting syndrome (PMWS)-affected and non-PMWS-affected pigs in Spain. *J Gen Virol* **87**, 833–837.

Kekarainen, T., Martínez-Guinó, L. & Segalés, J. (2009). Swine Torque teno virus detection in pig commercial vaccines, enzymes for laboratory use and human drugs containing components of porcine origin. *J Gen Virol* **90**, 648–653.

Kooistra, K., Zhang, Y.-H., Henriquez, N. V., Weiss, B., Mumberg, D. & Noteborn, M. H. M. (2004). TT virus-derived apoptosis-inducing protein induces apoptosis preferentially in hepatocellular carcinoma-derived cells. *J Gen Virol* **85**, 1445–1450.

Kopito, R. R. (2000). Aggresomes, inclusion bodies and protein aggregation. *Trends Cell Biol* **10**, 524–530.

Leppik, L., Gunst, K., Lehtinen, M., Dillner, J., Streker, K. & de Villiers, E. M. (2007). *In vivo* and *in vitro* intragenomic rearrangement of TT viruses. *J Virol* **81**, 9346–9356.

Mankertz, A. & Hillenbrand, B. (2001). Replication of porcine circovirus type 1 requires two proteins encoded by the viral rep gene. *Virology* **279**, 429–438.

Mankertz, A., Caliskan, R., Hattermann, K., Hillenbrand, B., Kurzendoerfer, P., Mueller, B., Schmitt, C., Steinfeldt, T. & Finsterbusch, T. (2004). Molecular biology of porcine circovirus: analyses of gene expression and viral replication. *Vet Microbiol* **98**, 81–88.

Martínez, L., Kekarainen, T., Sibila, M., Ruiz-Fons, F., Vidal, D., Gortázar, C. & Segalés, J. (2006). Torque teno virus (TTV) is highly prevalent in the European wild boar (*Sus scrofa*). *Vet Microbiol* **118**, 223–229.

Müller, B., Maerz, A., Doberstein, K., Finsterbusch, T. & Mankertz, A. (2008). Gene expression of the human Torque teno virus isolate P/1C1. *Virology* **381**, 36–45.

Mushahwar, I. K., Erker, J. C., Muerhoff, A. S., Leary, T. P., Simons, J. N., Birkenmeyer, L. G., Chalmers, M. L., Pilot-Matias, T. J. & Dexai, S. M. (1999). Molecular and biophysical characterization of TT virus: evidence for a new virus family infecting humans. *Proc Natl Acad Sci U S A* **96**, 3177–3182.

Nakai, K. & Horton, P. (1999). PSORT: a program for detecting sorting signals in proteins and predicting their subcellular localization. *Trends Biochem Sci* **24**, 34–36.

Niel, C., Diniz-Mendes, L. & Devalle, S. (2005). Rolling-circle amplification of Torque teno virus (TTV) complete genomes from human and swine sera and identification of a novel swine TTV genogroup. *J Gen Virol* **86**, 1343–1347.

Nishizawa, T., Okamoto, H., Konishi, K., Yoshizawa, H., Miyakawa, Y. & Mayumi, M. (1997). A novel DNA virus (TTV) associated with elevated transaminase levels in posttransfusion hepatitis of unknown etiology. *Biochem Biophys Res Commun* **241**, 92–97.

Okamoto, H. (2009). History of discoveries and pathogenicity of TT viruses. *Curr Top Microbiol Immunol* **331**, 1–20.

Okamoto, H., Akahane, Y., Ukita, M., Fukuda, M., Tsuda, F., Miyakawa, Y. & Mayumi, M. (1998). Fecal excretion of a nonenveloped DNA virus (TTV) associated with posttransfusion non-A-G hepatitis. *J Med Virol* **56**, 128–132.

Okamoto, H., Nishizawa, T., Tawara, A., Takahashi, M., Kishimoto, J., Sai, T. & Sugai, Y. (2000). TT virus mRNAs detected in the bone marrow cells from an infected individual. *Biochem Biophys Res Commun* **279**, 700–707.

Okamoto, H., Takahashi, M., Nishizawa, T., Tawara, A., Fukai, K., Muramatsu, U., Naito, Y. & Yoshikawa, A. (2002). Genomic characterization of TT viruses (TTVs) in pigs, cats and dogs and their relatedness with species-specific TTVs in primates and tupaias. *J Gen Virol* **83**, 1291–1297.

Qiu, J., Kakkola, L., Cheng, F., Ye, C., Söderlund-Venermo, M., Hedman, K. & Pintel, D. J. (2005). Human circovirus TT virus genotype 6 expresses six proteins following transfection of a full-length clone. *J Virol* **79**, 6505–6510.

Segalés, J., Martínez-Guinó, L., Cortey, M., Navarro, N., Huerta, E., Sibila, M., Pujols, J. & Kekarainen, T. (2009). Retrospective study on swine Torque teno virus genogroups 1 and 2 infection from 1985 to 2005 in Spain. *Vet Microbiol* **134**, 199–207.

Spector, D. L. & Lamond, A. I. (2011). Nuclear speckles. *Cold Spring Harb Perspect Biol* **3**, a000646.

Taira, O., Ogawa, H., Nagao, A., Tuchiya, K., Nunoya, T. & Ueda, S. (2009). Prevalence of swine Torque teno virus genogroups 1 and 2 in Japanese swine with suspected post-weaning multisystemic wasting syndrome and porcine respiratory disease complex. *Vet Microbiol* **139**, 347–350.

Wileman, T. (2007). Aggresomes and pericentriolar sites of virus assembly: cellular defense or viral design? *Annu Rev Microbiol* **61**, 149–167.

Zheng, H., Ye, L., Fang, X., Li, B., Wang, Y., Xiang, X., Kong, L., Wang, W., Zeng, Y. & other authors (2007). Torque teno virus (SANBAN isolate) ORF2 protein suppresses NF-κB pathways via interaction with IκB kinases. *J Virol* **81**, 11917–11924.